Universal local pair correlations of Lieb-Liniger bosons at quantum criticality

M.-S. Wang,[1,2] J.-H. Huang,[1] C.-H. Lee,[1] X.-G. Yin,[3] X.-W. Guan,[4,5] and M. T. Batchelor[5,6]

[1]*State Key Laboratory of Optoelectronic Materials and Technologies, School of Physics and Engineering,*
Sun Yat-Sen University, Guangzhou 510275, China
[2]*Department of Physics, Ludong University, Yantai 266000, China*
[3]*Division of Materials Science, Nanyang Technological University, Singapore 639798*
[4]*Wuhan Institute of Physics and Mathematics, Chinese Academy of Sciences, Wuhan 430071, China*
[5]*Department of Theoretical Physics, Research School of Physics and Engineering,*
Australian National University, Canberra ACT 0200, Australia
[6]*Mathematical Sciences Institute, Australian National University, Canberra ACT 0200, Australia*

The one-dimensional Lieb-Liniger Bose gas is a prototypical many-body system featuring universal Tomonaga-Luttinger liquid (TLL) physics and free fermion quantum criticality. We analytically calculate finite temperature local pair correlations for the strong-coupling Bose gas at quantum criticality using the polylog function in the framework of the Yang-Yang thermodynamic equations. We show that the local pair correlation has the universal value $g^{(2)}(0) \approx 2p/(n\varepsilon)$ in the quantum critical regime, the TLL phase, and the quasiclassical region, where p is the pressure per unit length rescaled by the interaction energy $\varepsilon = \frac{\hbar^2}{2m}c^2$ with interaction strength c and linear density n. This suggests the possibility to test finite temperature local pair correlations for the TLL in the relativistic dispersion regime and to probe quantum criticality with the local correlations beyond the TLL phase. Furthermore, thermodynamic properties at high temperatures are obtained by both high temperature and virial expansion of the Yang-Yang thermodynamic equation.

I. INTRODUCTION

Advances in the trapping and cooling of atoms in optical waveguides have opened up exciting possibilities for testing theory in low-dimensional quantum systems. Observed results to date are seen to be in excellent agreement with results obtained using the mathematical methods and analysis of exactly solved models [1–3]. These include the remarkable experimental realization of the Tonks-Girardeau gas [4–6], the super Tonks-Girardeau gas [7], Yang-Yang thermodynamics on an atom chip [8], and the phase diagram of the attractive Fermi gas [9]. Such exquisite tunability with tightly confined ultracold atoms provides unprecedented opportunities for improving our understanding of novel quantum phenomena such as quantum criticality, universal scaling theory, spin-charge separation and Tomonaga-Luttinger liquid (TLL) physics.

The one-dimensional (1D) delta-function interacting Lieb-Liniger Bose gas [1] is a many-body system solved exactly by the Bethe ansatz hypothesis. It has had a tremendous impact as an archetypical system in quantum statistical mechanics [10]. It's R matrix [11] provides the simplest solution of the Yang-Baxter equation [12]. Yang and Yang [13] showed that the thermodynamics of Lieb-Liniger bosons can be determined from the minimization of the Gibbs free energy subject to the Bethe ansatz equations [14,15]. This thermodynamic Bethe ansatz (TBA) method has been extended to a wide range of 1D quantum many-body systems [15]. In particular, Yang-Yang thermodynamics is fundamental to the Y system which has emerged as a ubiquitous integrable structure in mathematical physics [16]. In the present context, it provides the framework to study thermodynamics, quantum criticality, and TLL physics. The equation of state for Lieb-Liniger bosons has been obtained [17] analytically for strong coupling and low temperature in terms of the polylog function. The expression

for the equation of state in this regime enables the exploration of TLL physics and quantum criticality in this system.

In a recent experiment [18], thermal fluctuations were studied in a highly elongated weakly interacting Bose gas at high temperatures, where the quantum fluctuations are strongly suppressed. In this regime, the measured thermal fluctuations are in good agreement with the exact Yang-Yang thermodynamics. However, at quantum criticality, where the temperature is very low and interaction is very strong, quantum fluctuations are strongly enhanced. Towards the quantum critical regime, phonon fluctuations have been observed in the regime where the temperature is less than the chemical potential [19]. It is of particular interest to understand quantum correlations and fluctuations at quantum criticality. A finite temperature quantum phase transition does not exist in the 1D Lieb-Liniger Bose gas. However, there is a critical point in the grand canonical ensemble, when the chemical potential $\mu_c = 0$, which separates the vacuum from a filled "Fermi sea" of particles at zero temperature. At finite temperatures, a TLL with relativistic dispersions can be sustained in a region of the T-μ plane. This implies that for temperatures below a crossover value T^*, the low-lying excitations have a linear relativistic dispersion relation. If the temperature exceeds this crossover value, the excitations involve free quasiparticles with nonrelativistic dispersion. This crossover temperature can be identified from the breakdown of linear temperature-dependent entropy (see Fig. 1). In this phase diagram, quantum criticality is in the regime where $t = k_B T/(\frac{\hbar^2}{2m}c^2)$ is small, but $k_B T > |\mu - \mu_c|$, or for the temperature below the degenerate temperature $k_B T < \frac{\hbar^2}{2m}n^2$. Here k_B is the Boltzmann constant.

The local two-body (pair) correlations have been analytically calculated for a few limiting cases at $T = 0$ [20] and at finite temperatures for the TLL phase from the Yang-Yang
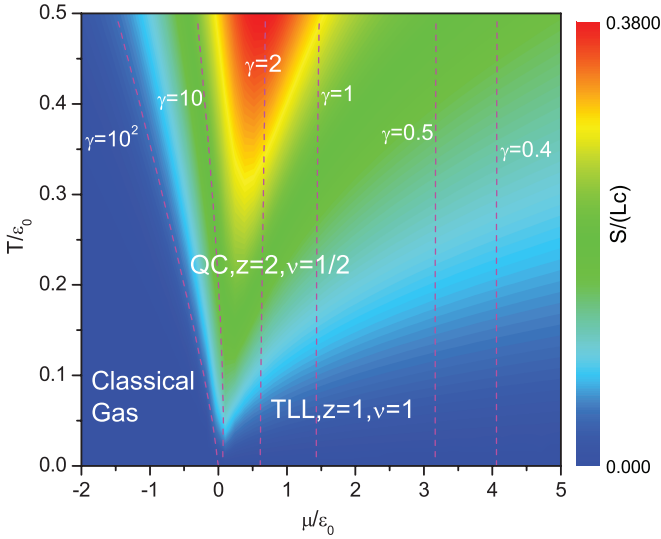
FIG. 1. (Color online) Quantum phase diagram of Lieb-Liniger bosons. The plot shows the dimensionless entropy in the T-μ plane obtained from the Yang-Yang thermodynamics (3), with $\varepsilon_0 = \frac{\hbar^2}{2m}c^2$. A crossover temperature separates the TLL critical phase with dynamic exponent $z = 1$ and correlation length exponent $\nu = 1$ from the quantum critical regime (QC) with exponents $z = 2$ and $\nu = 1/2$ near the critical point $\mu_c = 0$. Another crossover temperature separates the quasiclassical gas from the quantum critical regime. The red dashed lines indicate the values of the dimensionless coupling strength γ.

thermodynamic equations [21–25]. However, the local pair correlations have not been derived in the quantum critical regime. Moreover, it is very interesting to find an intrinsic relation between the local pair correlation and the equation of state. In principle, the Yang-Yang thermodynamic equations enable the numerical calculation of the local pair correlations in the whole parameter space. The local pair correlations are related to the universal contact which measures the probability of two bosons (or two fermions with opposite spins) at the same position [26–28].

In the present paper, we calculate the local pair correlations of Lieb-Liniger bosons in analytic fashion from the Yang-Yang thermodynamic equations using the polylog function in order to understand universal features of quantum fluctuations and critical phenomena in an archetypical quantum system. The local pair correlation is discussed in the T-μ phase diagram in terms of quantum criticality. In addition, a high-temperature expansion of the Yang-Yang thermodynamic equations is obtained in the strong-coupling regime. This allows one to extract the contributions from quantum and thermal fluctuations to the classical Boltzmann gas at high temperatures.

II. MODEL AND EQUATION OF STATE

The Hamiltonian

$$\mathcal{H} = -\frac{\hbar^2}{2m}\sum_{i=1}^{N}\frac{\partial^2}{\partial x_i^2} + g_{1D}\sum_{1\leqslant i < j\leqslant N}\delta(x_i - x_j) \quad (1)$$

of the Lieb-Liniger Bose gas [1] describes N spinless bosons with mass m constrained by periodic boundary conditions on a line of length L. The contact interactions are governed by the

effective 1D coupling constant $g_{1D} = -2\hbar^2/(ma_{1D})$, where $a_{1D} = (-a_\perp^2/2a_s)[1 - C(a_s/a_\perp)]$ is the 1D scattering length with $a_\perp = \sqrt{2\hbar/m\omega_\perp}$ and the numerical constant $C \approx 1.4603$ [29]. The dimensionless interaction strength is defined by $\gamma = c/n$ with $c = -2/a_{1D}$, where $n = N/L$ is the linear density. The interaction strength can be controlled by tuning either $\omega_\perp$ or a_s in experiments.

In describing the thermodynamics of the model the key quantity is the dressed energy

$$\epsilon(k) = T\,\ln[\rho^h(k)/\rho(k)] \quad (2)$$

which plays the role of excitation energy measured from the energy level $\epsilon(k_F) = 0$, where k_F is the Fermi-like momentum. The thermodynamics of the model in equilibrium follows from the Yang-Yang equation [13]

$$\epsilon(k) = \epsilon^0(k) - \mu - T\int_{-\infty}^{\infty}dq\,a_2(k-q)\ln(1 + e^{-\epsilon(q)/T}), \quad (3)$$

where $\epsilon^0(k) = \frac{\hbar^2}{2m}k^2$ is the bare dispersion, μ is the chemical potential, and

$$a_2(x) = \frac{1}{2\pi}\frac{2c}{c^2 + x^2}. \quad (4)$$

The pressure $p(T)$ and the free energy $F(T)$ are given in terms of the dressed energy by

$$p(T) = \frac{T}{2\pi}\int_{-\infty}^{\infty}dk\,\ln(1 + e^{-\epsilon(k)/T}), \quad (5)$$

$$F(T) = \mu n - \frac{T}{2\pi}\int_{-\infty}^{\infty}dk\,\ln(1 + e^{-\epsilon(k)/T}). \quad (6)$$

The pressure of the strongly coupled gas at finite temperatures has been obtained from (3) in the form [17]

$$p \approx -\sqrt{\frac{m}{2\pi\hbar^2}}T^{3/2}\,\mathrm{Li}_{3/2}(-e^{A/T})\left[1 - \frac{p}{\hbar^2c^3/(2m)}\right], \quad (7)$$

where Li_s is the standard polylog function and

$$A = \mu + \frac{2\,p(T)}{c} + \frac{1}{2\sqrt{\pi}c^3}\frac{T^{5/2}}{\left(\frac{\hbar^2}{2m}\right)^{3/2}}\mathrm{Li}_{5/2}(-e^{A_0/T}). \quad (8)$$

Furthermore, the Yang-Yang equation (3) can be expanded in powers of the dimensionless temperature $t = k_B T/\varepsilon_0$ with $\varepsilon_0 = (\frac{\hbar^2}{2m}c^2)$. Thus from (7) the dimensionless pressure $\tilde{p} = p/(\varepsilon_0 c)$ at finite temperatures follows as

$$\tilde{p} \approx -\frac{t^{3/2}}{2\sqrt{\pi}}\mathrm{Li}_{3/2}(-e^{\tilde{A}/t})\left[1 + \frac{t^{3/2}}{2\sqrt{\pi}}\mathrm{Li}_{3/2}(-e^{\tilde{A}/t})\right] \quad (9)$$

with

$$\tilde{A} = \tilde{\mu} - \frac{t^{3/2}}{\sqrt{\pi}}\mathrm{Li}_{3/2}(-e^{\tilde{A}_0/t}) + \frac{t^{5/2}}{2\sqrt{\pi}}\mathrm{Li}_{5/2}(-e^{\tilde{A}_0/t}) \quad (10)$$

and

$$\tilde{A}_0 = \tilde{\mu} - \frac{t}{\sqrt{\pi}}\mathrm{Li}_{3/2}(-e^{\tilde{\mu}/t}). \quad (11)$$

The result (9) is essentially a high-precision equation of state for Lieb-Liniger bosons at quantum criticality. We will verify that it is also valid for the high-temperature regime as long as $k_B T \ll \varepsilon$. Recalling the phase diagram Fig. 1,

the density and the compressibility can be cast into universal scaling forms [17,30–33]

$$n(T,\mu) - n_0(T,\mu) \approx t^{(d/z)+1-(1/\nu z)} \mathcal{F}\left(\frac{\mu - \mu_c}{t^{1/\nu z}}\right), \quad (12)$$

$$\kappa(T,\mu) - \kappa_0(T,\mu) \approx t^{(d/z)+1-(2/\nu z)} \mathcal{Q}\left(\frac{\mu - \mu_c}{t^{1/\nu z}}\right) \quad (13)$$

near the quantum critical point $\mu_c = 0$. Here the dynamic exponent $z = 2$ and the correlation length exponent $\nu = 1/2$ with the scaling functions given by

$$\mathcal{F}(x) = -\frac{c}{2\sqrt{\pi}} \text{Li}_{1/2}(-e^x), \quad (14)$$

$$\mathcal{Q}(x) = -\frac{c}{2\varepsilon\sqrt{\pi}} \text{Li}_{-1/2}(-e^x) \quad (15)$$

for $t > |\mu - \mu_c|$ in dimensionless units. The background density and compressibility in the vacuum are zero, i.e., $n_0(t,\mu) = \kappa_0(t,\mu) = 0$. These analytical results provide insight into quantum fluctuations near the quantum critical point. We will further demonstrate that the finite temperature local pair correlations shed light on quantum critical behavior.

The thermodynamic Bethe ansatz equations (3) provide a grand canonical description of the system (1), where the chemical potential is fixed. Usually, the Lieb-Liniger gas is discussed in the canonical ensemble, i.e., the particle number is fixed.

In fact, the thermodynamics of a canonical ensemble can be determined from the standard thermodynamic relation $n = (\partial p/\partial \mu)$, where the pressure per unit length is given by (5).

However, in an experiment the quantum gas with fixed number of particles is usually trapped by an external harmonic potential. The trapped density varies smoothly along the axial direction, with the density distribution read off from the local density function $n(x)$.

Each infinitely small interval around $n(x)$ can be reviewed as a grand canonical ensemble of the 1D integrable system. At equilibrium, the thermodynamics of each interval requests $de(x) = -p dL + \mu dN$. Through minimization of the total energy of the gas trapped in the external potential $E = \int e(x)dx + \int n(x)V(x)dx$, one can obtain the thermodynamic condition for equilibrium [34]

$$\mu + V(x) + \lambda = 0 \quad (16)$$

with $V(x)$ the external trapping potential and λ the Lagrange multiplier. This equilibrium condition is nothing but the local density approximation. For the Bose gas in a 1D harmonic trap, we thus obtain its density distribution from the equation of state within local density approximation [35,36].

Within the local density approximation, the chemical potentials in the equation of state (7) as well as in the TBA equations (3) are replaced by the local chemical potentials given by

$$\mu(x) = \mu(0) - V(x). \quad (17)$$

Here the external potential is defined as $V(x) = m\omega^2 x^2/2$ with harmonic frequency ω and the characteristic length for the harmonic trap is $a = \sqrt{\hbar/m\omega}$. In this setting, Eq. (17) can be alternatively written as

$$\mu(y)/\varepsilon_0 = \mu(0)/\varepsilon_0 - y^2 \quad (18)$$
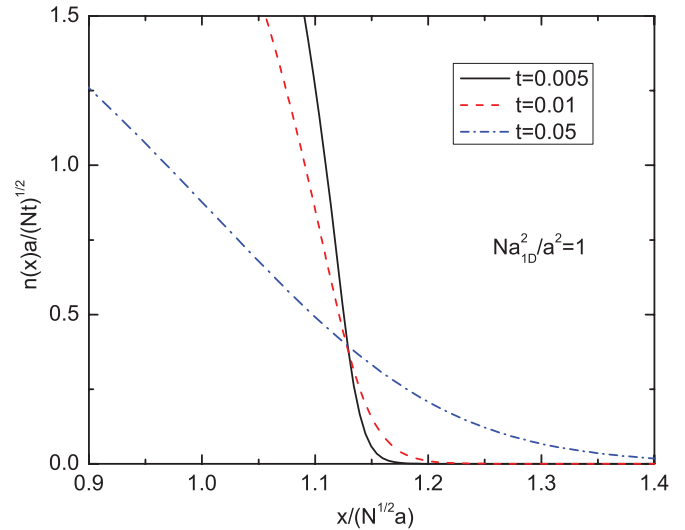

FIG. 2. (Color online) The density n vs normalized position at different temperatures for fixing $Na_{1D}^2/a^2 = 1$. The intersection point maps out the zero-temperature critical point at which the phase transition from the vacuum to the filled Bose gas occurs in the harmonic trap. Here $t = T/\varepsilon_0$.

in which the dimensionless coordinate $y = x/(a^2 c)$. In terms of dimensionless units, the dimensionless density n/c can be obtained for fixed dimensionless chemical potential μ/ε_0. The total particle number N is obtained from the relation

$$\frac{Na_{1D}^2}{a^2} = 4 \int_{-\infty}^{\infty} n(y)/c \, dy \quad (19)$$

with the 1D scattering length $a_{1D} = -2/c$. For fixed value of trapping center chemical potential $\mu(0)/\varepsilon_0$, we may determine the value Na_{1D}^2/a^2.

In turn, for different values of Na_{1D}^2/a^2, i.e., for fixed particle number, the thermodynamic properties can be mapped out through the density profiles of the trapped gas at finite temperatures. E.g., in Fig. 2, we show the scaled density distributions of bosons in the harmonic trap for $Na_{1D}^2/a^2 = 1$ at different temperatures. It is clearly seen that the density curves at different temperatures intersect at a common point. We read off the dynamic exponent $z = 2$ and the correlation length exponent $\nu = 1/2$ from the universal scaling function (12) within the local density approximation.

III. LOCAL PAIR CORRELATIONS

The general calculation of correlation functions in quantum many-body systems is a notoriously difficult problem, even more so at finite temperature [14]. Fortunately the two-particle local pair correlation $g^{(2)}(0)$ can be calculated relatively easily from the free energy. In the grand canonical description, the Hellmann-Feynman theorem gives

$$g^{(2)}(0) := \langle \Psi^\dagger \Psi^\dagger \Psi \Psi \rangle = \frac{2m}{\hbar^2 n}\left(\frac{\partial f}{\partial c}\right)_{n,t}, \quad (20)$$

where $f = \mu - p/n$ is the free energy per particle. For constant n the local pair correlations require the calculation of the derivatives $\partial\mu/\partial c$ and $\partial p/\partial c$, which can be done by

iteration. Using the result (7) we find

$$\frac{\partial p}{\partial c} \approx -\sqrt{\frac{mT}{2\pi\hbar^2}} \mathrm{Li}_{3/2}(-e^{A/T}) \left[1 - \frac{2p}{\hbar^2 c^3/(2m)}\right] \frac{\partial A}{\partial c}, \quad (21)$$

where $\partial A/\partial c$ can be calculated from (10) by iteration. The calculation of $\partial\mu/\partial c$ is cumbersome. To this end, we first find the explicit form of the density $n = \partial p/\partial\mu$ and then take the derivative with respective to c. After a lengthy iteration, we find

$$\frac{\partial\mu}{\partial c} \approx -\sqrt{\frac{2m}{\pi\hbar^2}} \frac{T^{3/2}}{c^2} \left\{ \frac{\mathrm{Li}_{1/2}(-e^{A/T})^2}{\mathrm{Li}_{-1/2}(-e^{A/T})} \right.$$
$$\times \left[1 + \frac{1}{c}\sqrt{\frac{2mT}{\pi\hbar^2}} \mathrm{Li}_{1/2}(-e^{A/T}) - \frac{6mT}{c^2\pi\hbar^2} \mathrm{Li}_{1/2}(-e^{A/T})^2\right]$$
$$\left. + \mathrm{Li}_{3/2}(-e^{A/T})\left[1 - \frac{12mT}{c^2\pi\hbar^2} \mathrm{Li}_{1/2}(-e^{A/T})^2\right] \right\}. \quad (22)$$

Finally, from expressions (21) and (22), we obtain the local pair correlations in the form

$$g^{(2)}(0) \approx -\frac{\gamma t^{3/2}}{\sqrt{\pi}} \mathrm{Li}_{3/2}(-e^{\tilde{A}/t}) \left[1 - \frac{11t}{\pi} \mathrm{Li}_{1/2}(-e^{\tilde{A}/t})\right], \quad (23)$$

where $\tilde{A}$ is given by (10).

We note that the local pair correlations satisfy a simple relation

$$g^{(2)}(0) = \frac{2p}{n\varepsilon} + O\left(\frac{1}{\gamma^4}\right), \quad (24)$$

where t is small. It turns out that this simple looking result not only holds for the quantum critical regime, but also for the TLL phase and the ground state at $T = 0$. In this sense it is a universal relation. The low-temperature local correlation for the TLL phase follows from (24) as

$$g^{(2)}(0) = \frac{4\pi^2}{3\gamma^2}\left[1 - \frac{6}{\gamma} + \frac{T^2}{4\pi^2\left(\frac{\hbar^2}{2m}n^2\right)^2}\right] + O\left(\frac{1}{\gamma^4}\right), \quad (25)$$

which coincides with the result given in [21–24].

Figure 3 shows a plot of the local pair correlations obtained from (23) in comparison with the numerical result. The
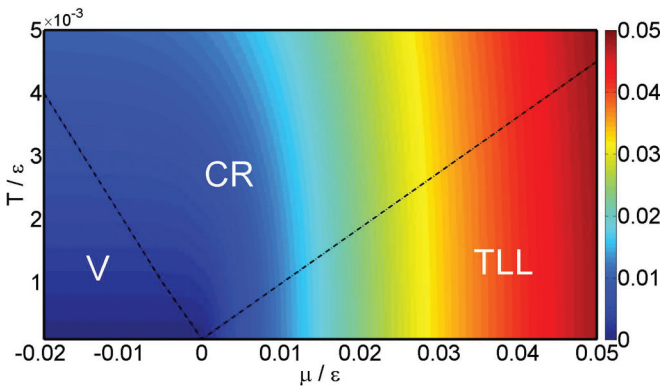

FIG. 3. (Color online) Local pair correlation $g^{(2)}(0)$ at low temperatures in the t-μ plane. The black lines denote the crossover temperature separating the TLL phase from the quantum critical regime (CR) and the vacuum (V) from the quantum critical regime (CR).
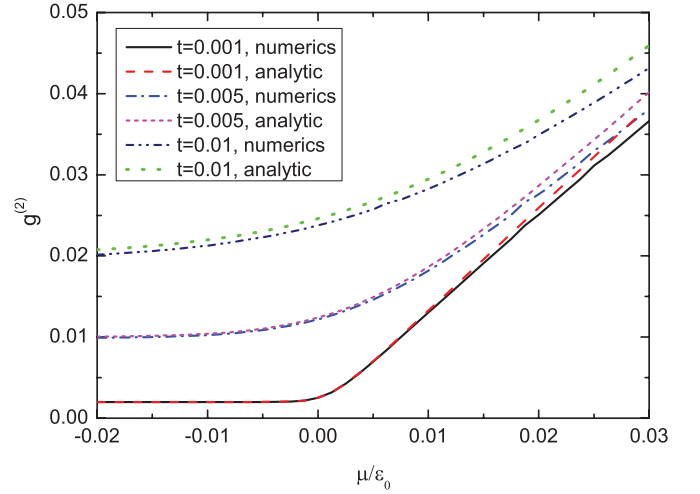

FIG. 4. (Color online) Local pair correlation $g^{(2)}(0)$ vs chemical potential at quantum criticality. The correlation function $g^{(2)}(0)$ at different temperature values shows good agreement between the analytical relation (24) and the numerical result obtained from the TBA equation (3).

crossover temperatures, which separate the quantum critical regime from the TLL, are determined by the breakdown of the TLL with the local correlation (25). The crossover line is consistent with the phase diagram Fig. 1. The TLL phase persists below the crossover temperatures, where both results (24) and (25) coincide (see Fig. 3). This represents a smooth crossover from the relativistic TLL regime to the regime governed by a nonrelativistic dispersion relation. The local correlations increase as the chemical potential becomes large and positive because of the decrease of the interaction. The temperature enhances the local pair correlations (see Fig. 4). We see clearly that the local correlations (24) cover the quantum critical region, the TLL phase, and ground state at $T = 0$.

For nonzero temperature, the vacuum can be taken as a semiclassical gas regime, where the particle density $n \sim \frac{1}{\lambda}e^{-|\mu|/T}$ with thermal wavelength $\lambda^{-1} = \sqrt{mk_BT/2\pi\hbar^2}$, which is much smaller than the mean distance between two particles. The local pair correlation tends to zero. We see that the relation (24) between the local correlations and pressure holds in the physical regime as long as the temperature is below the degenerate temperature and $T \ll \frac{\hbar^2}{2m}c^2$. Near the critical point $\mu_c = 0$, the density is very low, therefore the interaction is strong and sits in the Tonks-Giraradau regime. At high temperatures, this crossover disappears due to suppression of the quantum fluctuations. At high temperatures, the chemical potential becomes more negative. We consider this limit in the next section.

IV. HIGH-TEMPERATURE EXPANSION

The recent measurements [18] on thermal fluctuations in the 1D Bose gas were carried out in the weak-coupling and high-temperature regimes. The variance of atom number $\langle \delta N^2 \rangle$ in a volume Δ can be evaluated as [18]

$$\langle \delta N^2 \rangle = \Delta k_B T \left(\frac{\partial n(\mu, T)}{\partial \mu}\right)_T, \quad (26)$$

where the local density $n(\mu, T)$ can be determined from the equation of state in the thermodynamic limit. In particular, Armijo [19] has recently observed the quantum phonon fluctuations in the 1D Bose gas using *in situ* absorption imaging and statistical analysis of the density profiles. This opens up further study of quantum vacuum fluctuations in a finite Lieb-Liniger Bose gas.

Here we first consider the equation of state of this system at high temperatures and in strong-coupling regimes. At high temperatures, the TBA equation (3) can be expanded in an appropriate form. For convenience, we define the function $\eta(k) = e^{\epsilon(k)/T}$ and the inverse temperature parameter $\alpha = \hbar^2 c^2/(2mT)$. The TBA equation (3) can then be written

$$\eta^{-1}(k) = x_k \exp\left\{\int_{-\infty}^{\infty} dq \, a_2(k-q) \ln[1 + \eta^{-1}(q)]\right\}, \quad (27)$$

where $x_k = e^{[\mu - \epsilon_0(k)]/T} \ll 1$ at high temperatures. We carry out an expansion of this equation in powers of $Z = e^{\mu/T} \ll 1$ as $T \to \infty$. Collecting the first few terms, we have

$$\eta^{-1}(k) \approx x_k(1 + B_1 Z + B_2 Z^2 + B_3 Z^3) + O(Z^5), \quad (28)$$

where the coefficients B_i, for finite α, are given by

$$B_1 = \frac{c}{(c^2 + k^2)\sqrt{\alpha\pi}},$$

$$B_2 = \frac{1}{(c^2 + k^2)\alpha\pi} + \frac{c^2}{2(c^2 + k^2)^2\alpha\pi} - \frac{c}{2\sqrt{2}(c^2 + k^2)\sqrt{\alpha\pi}},$$

$$B_3 = \frac{c}{(c^2 + k^2)^2(\alpha\pi)^{3/2}} + \frac{c^3}{6(c^2 + k^2)^3(\alpha\pi)^{3/2}}$$
$$- \frac{1}{\sqrt{2}(c^2 + k^2)\alpha\pi} - \frac{c^2}{2\sqrt{2}(c^2 + k^2)^2\alpha\pi}. \quad (29)$$

Using the expansion (28) gives the pressure (5) in the asymptotic form

$$p = \sqrt{\frac{m}{2\pi\hbar^2}} T^{-3/2} Z[1 + f_1 Z + f_2 Z^2 + f_3 Z^3] + O(Z^5), \quad (30)$$

with

$$f_1 = e^{\alpha}[1 - \text{Erf}(\sqrt{\alpha})] - \frac{1}{2\sqrt{2}},$$

$$f_2 = e^{\alpha}[1 - \text{Erf}(\sqrt{\alpha})]\left(\frac{5}{4\sqrt{\pi\alpha}} - \frac{\sqrt{\alpha}}{2\sqrt{\pi}} - \frac{1}{2\sqrt{2}}\right)$$
$$- e^{2\alpha}[1 - \text{Erf}(\sqrt{2\alpha})] + \frac{1}{2\pi} + \frac{1}{3\sqrt{3}},$$

$$f_3 = \frac{9}{8\pi^{3/2}\sqrt{\alpha}} - \frac{\sqrt{\alpha}}{12\pi^{3/2}} - \frac{1}{2\sqrt{2\pi}} - \frac{\sqrt{2}}{\pi}$$
$$+ e^{\alpha}[1 - \text{Erf}(\sqrt{\alpha})]\left(\frac{1}{2\pi^{3/2}\alpha} - \frac{11 - \alpha}{12\pi} + \frac{1}{16\pi\alpha}\right.$$
$$\left. - \frac{5}{4\sqrt{2\pi\alpha}} + \frac{\sqrt{\alpha}}{2\sqrt{2\pi}} + \frac{1}{3\sqrt{3}}\right)$$
$$+ e^{2\alpha}[1 - \text{Erf}(\sqrt{2\alpha})]\left(\frac{1}{2\sqrt{2}} - \frac{3}{2\sqrt{\pi\alpha}} - \frac{2\sqrt{\alpha}}{\sqrt{\pi}}\right)$$
$$+ e^{3\alpha}[1 - \text{Erf}(\sqrt{3\alpha})], \quad (31)$$

where $\text{Erf}(x)$ is the standard error function.

The TBA results reduce to several limiting cases. The pressure p_c of the classical Boltzmann gas

$$p_c = \sqrt{\frac{m}{2\pi\hbar^2}} T^{-3/2} e^{\mu/T} \quad (32)$$

follows in the limit $T \to \infty$. The pressure of the ideal Fermi gas

$$p = -\sqrt{\frac{m}{2\pi\hbar^2}} T^{3/2} \text{Li}_{3/2}(-e^{\mu/T}) \quad (33)$$

is obtained in the limit $c \to \infty$. Similarly the pressure of the ideal Bose gas

$$p = \sqrt{\frac{m}{2\pi\hbar^2}} T^{3/2} \text{Li}_{3/2}(e^{\mu/T}) \quad (34)$$

follows in the limit $c \to 0$.

In the high-temperature limit, the chemical potential tends to negative infinity. In this region, far away from criticality, the pressure (7) given in terms of the polylog function and the high-temperature expansion result (30) are highly accurate for $\alpha > 5$ (see Fig. 5). The polylog function result (7) gives a better fit with the numerical result obtained from the TBA (3) even for large values of $k_B T/\mu$. At high temperatures, although the thermal fluctuations dominate, the quantum statistics are still microscopically significant. The quantum statistical effect is evidenced from changing the value of α, which can be controlled in current experiments [18,19]. In the Tonks-Girardeau limit $\alpha \to \infty$ the gas approaches free fermions. For small values of α, i.e., in the weak-coupling region, we see the pressure (30) obtained from the high-temperature expansion is consistent with the numerical result at high temperatures (see Fig. 5). But as expected, the result (30) is no longer accurate for $\alpha \ll 1$.

In the weak-coupling limit and at high temperatures it is more practical to consider a virial expansion with the TBA equation (3), i.e.,

$$p\sqrt{\frac{2\pi\hbar^2}{m}} T^{3/2} = \text{Li}_{3/2}(Z) + \sqrt{2} \, p_2 Z^2 + O(Z^3) \quad (35)$$
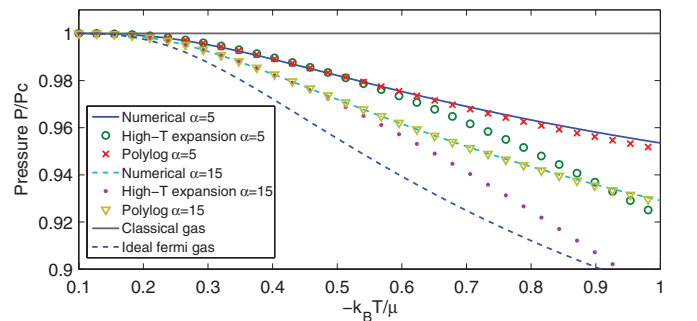

FIG. 5. (Color online) The ratio of the pressure p/p_c vs $k_B T/\mu$ at high temperatures for $\alpha = 5$ and 15. Here p_c is the pressure of the classical Boltzmann gas. High accuracy of the pressure (7) is seen for $-\infty < k_B T/\mu < 1$. At high temperatures both pressure (7) obtained from the polylog formalism and the one (30) obtained from high-temperature expansion are accurate by comparing with the numerical result from the TBA equation (3). The polylog formalism is also valid at low temperatures as long as $\alpha \gg 1$.
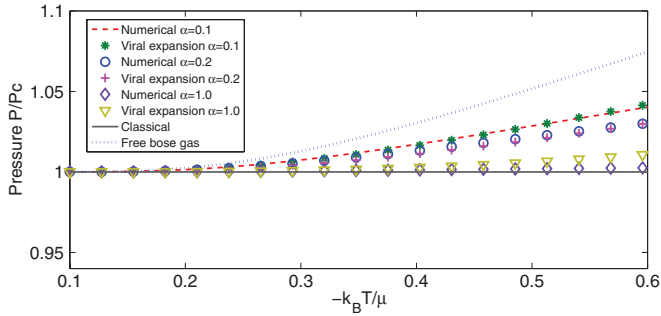
FIG. 6. (Color online) Comparison between different values for the pressure p/p_c vs $k_B T/\mu$ at high temperatures for $\alpha = 0.1, 0.2, 1.0$. For small values of α, the pressure (35) obtained from the virial expansion is in good agreement with the result obtained from the numerical solution of the TBA equation (3).

with $Z = \exp(\mu/T)$. The first term in the right-hand side of this equation comes from free bosons and

$$p_2 = -\frac{1}{2} - \frac{\exp(\alpha^2/2)}{2}[-1 + \mathrm{Erf}(\sqrt{\alpha/2})] \tag{36}$$

contributes to the second virial coefficient. From the comparison shown in Fig. 6, we see clearly that the pressure obtained from the virial expansion gives a high-precision equation of state for $\alpha < 1$. This result is valid for the experimental setting with $\alpha < 1$ [18,19].

V. CONCLUSION AND DISCUSSION

In conclusion, we have studied finite temperature local pair correlations of the Lieb-Liniger Bose gas at quantum criticality. A simple relation (24) between the local correlations and the pressure has been obtained in the framework of the Yang-Yang thermodynamic equations. This relation holds for both the quantum critical regime and the TLL phase at quantum criticality. It provides a simple way to probe finite temperature local pair correlations for the TLL over the whole relativistic dispersion regime and to test quantum criticality with the local correlations beyond the TLL phase. In the quantum critical regime, the thermal fluctuations strongly couple to

the quantum fluctuations with universal free fermion $z = 2$ quantum criticality. The local pair correlations provide insight into the microscopic quantum statistical effects at quantum criticality. We also derived the thermodynamic equations (30) and (35) of the Lieb-Liniger gas at high temperatures using a high-temperature expansion of the Yang-Yang thermodynamic equations. The effect of quantum statistics is microscopically significant even in the thermal fluctuation dominated high-temperature regime. In particular, the equation of state given by (35) is highly accurate for the weak-coupling and high-temperature regimes.

Our analytical prediction (24) for local pair correlations can be tested using current experimental techniques for preparing and detecting 1D gases. An ensemble of parallel 1D Bose gases can be prepared [5,6] by loading ultracold Bose atoms into a two-dimensional (2D) optical lattice. The 2D optical lattices, an ensemble of parallel 1D tubes, can be formed by superimposing two standing-wave lasers on the crossed dipole trap. The depth of the 2D lattice must be sufficiently large to make the quantum tunneling among these 1D tubes negligible. That is, atoms in these 1D tubes are almost all in the lowest transverse vibrational state. The photoassociation techniques for measuring local pair correlations in zero-temperature 1D Bose gases [6] could also be used to explore local pair correlations in nonzero temperature systems, such as the Lieb-Liniger Bose gas at quantum criticality studied in this paper. In particular, the universal relation between the local pair correlation and the pressure at quantum criticality could be explored following the experimental scheme for measuring the homogeneous contact of a unitary Fermi gas [37].

[1] E. H. Lieb and W. Liniger, Phys. Rev. **130**, 1605 (1963).
[2] M. Gaudin, Phys. Lett. A **24**, 55 (1967).
[3] C. N. Yang, Phys. Rev. Lett. **19**, 1312 (1967).
[4] B. Paredes, A. Widera, V. Murg, O. Mandel, S. Fölling, I. Cirac, G. V. Shlyapnikov, T. W. Hänsch, and I. Bloch, Nature (London) **429**, 277 (2004).
[5] T. Kinoshita, T. Wenger, and D. S. Weiss, Science **305**, 1125 (2004).
[6] T. Kinoshita, T. Wenger, and D. S. Weiss, Phys. Rev. Lett. **95**, 190406 (2005).
[7] E. Haller, M. Gustavsson, M. J. Mark, J. G. Danzl, R. Hart, G. Pupillo, and H.-C. Nägerl, Science **325**, 1224 (2009).
[8] A. H. van Amerongen, J. J. P. van Es, P. Wicke, K. V. Kheruntsyan, and N. J. van Druten, Phys. Rev. Lett. **100**, 090402 (2008).
[9] Y. Liao, A. S. C. Rittner, T. Paprotta, W. Li, G. B. Partridge, R. G. Hulet, S. K. Baur, and E. J. Mueller, Nature (London) **467**, 567 (2010).
[10] M. A. Cazalilla, R. Citro, T. Giamarchi, E. Orignac, and M. Rigol, Rev. Mod. Phys. **83**, 1405 (2011).
[11] J. B. McGuire, J. Math. Phys. **5**, 622 (1964).
[12] See, e.g., M. Jimbo, Int. J. Mod. Phys. A **4**, 3759 (1989).
[13] C. N. Yang and C. P. Yang, J. Math. Phys. **10**, 1115 (1969).
[14] V. E. Korepin, A. G. Izergin, and N. M. Bogoliubov, *Quantum Inverse Scattering Method and Correlation Functions* (Cambridge University Press, Cambridge, UK, 1993).
[15] M. Takahashi, *Thermodynamics of One-Dimensional Solvable Models* (Cambridge University Press, Cambridge, UK, 1999).
[16] A. Kuniba, T. Nakanishi, and J. Suzuki, J. Phys. A **44**, 103001 (2011).

[17] X.-W. Guan and M. T. Batchelor, J. Phys. A **44**, 102001 (2011).

[18] J. Armijo, T. Jacqmin, K. V. Kheruntsyan, and I. Bouchoule, Phys. Rev. Lett. **105**, 230402 (2010); Phys. Rev. A **83**, 021605(R) (2011).

[19] J. Armijo, Phys. Rev. Lett. **108**, 225306 (2012).

[20] D. M. Gangardt and G. V. Shlyapnikov, Phys. Rev. Lett. **90**, 010401 (2003).

[21] K. V. Kheruntsyan, D. M. Gangardt, P. D. Drummond, and G. V. Shlyapnikov, Phys. Rev. Lett. **91**, 040403 (2003); Phys. Rev. A **71**, 053615 (2005).

[22] M. A. Cazalilla, Phys. Rev. A **67**, 053606 (2003).

[23] X.-W. Guan, M. T. Batchelor, and M. Takahashi, Phys. Rev. A **76**, 043617 (2007).

[24] M. Kormos, G. Mussardo, and A. Trombettoni, Phys. Rev. Lett. **103**, 210404 (2009); Phys. Rev. A **81**, 043606 (2010).

[25] M. Kormos, Y.-Z. Chou, and A. Imambekov, Phys. Rev. Lett. **107**, 230405 (2011).

[26] S. Tan, Ann. Phys. (NY) **323**, 2952 (2008); **323**, 2971 (2008); **323**, 2987 (2008).

[27] M. Olshanii and V. Dunjko, Phys. Rev. Lett. **91**, 090401 (2003); M. Barth and W. Zwerger, Ann. Phys. (NY) **326**, 2544 (2011).

[28] P. Vignolo and A. Minguzzi, Phys. Rev. Lett. **110**, 020403 (2013).

[29] M. Olshanii, Phys. Rev. Lett. **81**, 938 (1998); V. Dunjko, V. Lorent, and M. Olshanii, *ibid.* **86**, 5413 (2001).

[30] M. P. A. Fisher, P. B. Weichman, G. Grinstein, and D. S. Fisher, Phys. Rev. B **40**, 546 (1989).

[31] S. Sachdev, *Quantum Phase Transitions* (Cambridge University Press, Cambridge, UK, 1999).

[32] Q. Zhou and T.-L. Ho, Phys. Rev. Lett. **105**, 245702 (2010).

[33] K. R. A. Hazzard and E. J. Mueller, Phys. Rev. A **84**, 013604 (2011).

[34] Z.-Q. Ma and C. N. Yang, Chin. Phys. Lett. **26**, 120506 (2009).

[35] A. Imambekov and E. Demler, Phys. Rev. A **73**, 021602 (2006); Ann. Phys. **321**, 2390 (2006).

[36] C. Menotti and S. Stringari, Phys. Rev. A **66**, 043610 (2002).

[37] Y. Sagi, T. E. Drake, R. Paudel, and D. S. Jin, Phys. Rev. Lett. **109**, 220402 (2012).